International Journal of Science and Engineering Applications
Volume 14-Issue 12, 12 – 20, 2025, ISSN:- 2319 - 7560
DOI: 10.7753/IJSEA1412.1003

Structural Analysis and Lightweight Optimization of an All-Terrain Vehicle Frame Based on the Finite Element Method

Xike Wang
School of Automotive Engineering,
Zibo Polytechnic University
Zibo, Shandong, China

Abstract: Based on the finite element method, this study investigates the structural optimization of an All-Terrain Vehicle (ATV) frame to achieve lightweight design. A three-dimensional model of the frame was established and subjected to static structural analysis under extreme load conditions, as well as modal analysis to determine its inherent vibration characteristics. The analysis results identified potential areas for improvement. An optimization design was then carried out, which successfully reduced the frame's mass while ensuring its strength and stiffness met the required standards. The results demonstrate the effectiveness of the proposed method in enhancing performance and achieving weight reduction..

Keywords: All-Terrain Vehicle (ATV); Frame; Finite Element Analysis; Static Analysis; Modal Analysis; Structural Optimization

1. INTRODUCTION

The frame is the core load-bearing structure of an All-Terrain Vehicle (ATV), whose performance is critical for safety and mobility in harsh environments. Traditional designs often face challenges in balancing structural strength with weight. This paper presents a concise study on the structural optimization of an ATV frame using the Finite Element Method (FEM). Through static and modal analysis, key areas for improvement are identified, leading to a proposed optimized design that achieves significant weight reduction while maintaining structural integrity, thereby enhancing overall vehicle performance.

2. ESTABLISHMENT OF 3D FRAME MODEL AND FINITE ELEMENT PRE-PROCESSING

Normal or Body TexEstablishment of the 3D Geometric Model

To perform an accurate finite element analysis, the first step is to create a geometric model of the frame. This study uses a space-frame structure from a typical tubular All-Terrain Vehicle as the prototype. To ensure computational efficiency and solution stability while preserving the mechanical characteristics of the primary load-bearing structure, necessary simplifications were applied to the original model:

Minor non-structural attachments, such as wire harness brackets and sensor mounts, were omitted.

Process features with negligible impact on overall stiffness, such as small chamfers and fillets, were suppressed.

Welded connections between steel tubes were treated as continuous, meaning components were directly connected during modeling without simulating the detailed geometry of the weld seams.

The simplified three-dimensional model was developed using SolidWorks software, as illustrated in Figure 1. This model accurately represents the main topological layout of the frame, including key components such as the main longitudinal rails, crossmembers, suspension mounting points, and engine mounts.

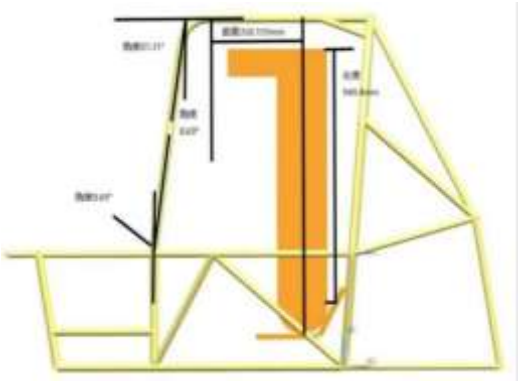

Figure. 1 Simplified three-dimensional mode

FINITE ELEMENT PRE-PROCESSING

The frame structure is constructed from Q235 carbon steel, a material commonly used in automotive structural components due to its favorable mechanical properties and cost-effectiveness. The material was modeled as linear-elastic and isotropic with properties as specified in Table 1. These parameters serve as the fundamental input for the subsequent structural simulations.

International Journal of Science and Engineering Applications
Volume 14-Issue 12, 12 – 20, 2025, ISSN:- 2319 - 7560
DOI: 10.7753/IJSEA1412.1003

Table 1: Material Properties of the Frame

Property	**Value**	**Unit**
Young's Modulus	210	GPa
Poisson's Ratio	0.3	-
Density	7850	kg/m³
Yield Strength	235	MPa
The discretization of the continuous geometry into finite elements was performed using shell elements (ANSYS SHELL181), which are particularly suitable for analyzing thin-walled structural components. This element formulation provides appropriate capabilities for capturing the bending and membrane stress states prevalent in the tubular frame structure.		

PropertyValue	**ValueUnitYoung's Modulus**210GPa**Poisson's Ratio**0.3-**Density**7850kg/m³**Yield Strength**235MPaThe discretization of the continuous geometry into finite elements was performed using shell elements (ANSYS SHELL181), which are particularly suitable for analyzing thin-walled structural components. This element formulation provides appropriate capabilities for capturing the bending and membrane stress states prevalent in the tubular frame structure.	**UnitYoung's Modulus**210GPa**Poisson's Ratio**0.3-**Density**7850kg/m³**Yield Strength**235MPaThe discretization of the continuous geometry into finite elements was performed using shell elements (ANSYS SHELL181), which are particularly suitable for analyzing thin-walled structural components. This element formulation provides appropriate capabilities for capturing the bending and membrane stress states prevalent in the tubular frame structure.
elements (ANSYS SHELL181), which are particularly suitable for analyzing thin-walled structural components. This element formulation provides appropriate capabilities for capturing the bending and membrane stress states prevalent in the tubular frame structure.	elements (ANSYS SHELL181), which are particularly suitable for analyzing thin-walled structural components. This element formulation provides appropriate capabilities for capturing the bending and membrane stress states prevalent in the tubular frame structure.	
Density7850kg/	7850kg/m³**Yiel**	kg/m³**Yield**

PropertyValue	**ValueUnitYoung's Modulus**210GPa**Poisson's Ratio**0.3-**Density**7850kg/m³**Yield Strength**235MPaThe discretization of the continuous geometry into finite elements was performed using shell elements (ANSYS SHELL181), which are particularly suitable for analyzing thin-walled structural components. This element formulation provides appropriate capabilities for capturing the bending and membrane stress states prevalent in the tubular frame structure.	**UnitYoung's Modulus**210GPa**Poisson's Ratio**0.3-**Density**7850kg/m³**Yield Strength**235MPaThe discretization of the continuous geometry into finite elements was performed using shell elements (ANSYS SHELL181), which are particularly suitable for analyzing thin-walled structural components. This element formulation provides appropriate capabilities for capturing the bending and membrane stress states prevalent in the tubular frame structure.
m³**Yield Strength**235MPaThe discretization of the continuous geometry into finite elements was performed using shell elements (ANSYS SHELL181), which are particularly suitable for analyzing thin-walled structural components. This element formulation provides appropriate capabilities for capturing the bending and	**d Strength**235MPaThe discretization of the continuous geometry into finite elements was performed using shell elements (ANSYS SHELL181), which are particularly suitable for analyzing thin-walled structural components. This element formulation provides appropriate capabilities for	**Strength**235MPaThe discretization of the continuous geometry into finite elements was performed using shell elements (ANSYS SHELL181), which are particularly suitable for analyzing thin-walled structural components. This element formulation provides appropriate capabilities for capturing the bending and membrane stress states prevalent in the tubular frame

PropertyValue	**ValueUnitYoung's Modulus**210GPa**Poisson's Ratio**0.3-**Density**7850kg/m³**Yield Strength**235MPaThe discretization of the continuous geometry into finite elements was performed using shell elements (ANSYS SHELL181), which are particularly suitable for analyzing thin-walled structural components. This element formulation provides appropriate capabilities for capturing the bending and membrane stress states prevalent in the tubular frame structure.	**UnitYoung's Modulus**210GPa**Poisson's Ratio**0.3-**Density**7850kg/m³**Yield Strength**235MPaThe discretization of the continuous geometry into finite elements was performed using shell elements (ANSYS SHELL181), which are particularly suitable for analyzing thin-walled structural components. This element formulation provides appropriate capabilities for capturing the bending and membrane stress states prevalent in the tubular frame structure.
membrane stress states prevalent in the tubular frame structure.	capturing the bending and membrane stress states prevalent in the tubular frame structure.	structure.
Yield Strength235MPaThe discretization of the continuous geometry into finite elements was performed using shell elements (ANSYS SHELL181), which are particularly suitable for analyzing thin-walled structural components. This element formulation provides appropriate capabilities for capturing the bending and membrane stress states prevalent in the tubular frame structure.	235MPaThe discretization of the continuous geometry into finite elements was performed using shell elements (ANSYS SHELL181), which are particularly suitable for analyzing thin-walled structural components. This element formulation provides appropriate capabilities for capturing the bending and membrane stress states prevalent in the tubular frame structure.	MPaThe discretization of the continuous geometry into finite elements was performed using shell elements (ANSYS SHELL181), which are particularly suitable for analyzing thin-walled structural components. This element formulation provides appropriate capabilities for capturing the bending and membrane stress states prevalent in the tubular frame structure.

The discretization of the continuous geometry into finite elements was performed using shell elements (ANSYS SHELL181), which are particularly suitable for analyzing thin-walled structural components. This element formulation provides appropriate capabilities for capturing the bending and membrane stress states prevalent in the tubular frame structure.

A comprehensive mesh convergence study was conducted to determine the optimal element size, balancing computational accuracy with processing requirements. The final mesh was generated with a global element size of 5 mm, resulting in a high-quality mesh comprising 125,483 nodes and 78,952 elements. The mesh quality was verified against standard metrics including element aspect ratio, skewness, and Jacobian, all of which were found to be within acceptable limits for reliable analysis.

All structural connections between tubular members were modeled as perfectly bonded interfaces, implemented through shared nodes at component junctions. This modeling approach represents an idealized welded condition, allowing complete transfer of both forces and moments between connected elements without relative displacement. Critical interface locations, particularly suspension attachment points and engine mounting positions, were explicitly identified during this process to facilitate the accurate application of boundary conditions and loads in subsequent analysis phases.

3. STATIC STRUCTURAL ANALYSIS

3.1 Determination of Load Cases

To comprehensively evaluate the structural integrity of the ATV frame, three critical and representative static load cases were defined, simulating severe operating conditions that induce maximum stress and deformation.

Case 1: Vertical Bending Case. This simulates the vehicle carrying its full weight on a flat surface. The total load was calculated based on the vehicle's curb weight, a driver's weight, and a safety factor. This load was distributed to the suspension mounting points.

Case 2: Torsional Case. This simulates the frame's resistance to twisting when one wheel is lifted, such as when traversing uneven terrain. This is a key scenario for assessing the frame's torsional stiffness. The analysis modeled the situation with one rear wheel raised, applying a corresponding moment to the frame.

Case 3: Combined Braking and Bending Case. This simulates the load during emergency braking. In addition to the vertical

load from the Bending Case, longitudinal forces were applied at the suspension points to replicate the deceleration inertia.

3.2 Application of Constraints and Loads

The constraints and loads were applied to the suspension mounting points to realistically represent the interaction between the frame and the vehicle's chassis systems.

Constraints: For all cases, the mounting points for the front suspension were constrained in all translational degrees of freedom. The rear suspension mounting points were constrained in the vertical and transverse directions but were left free in the longitudinal direction to allow for the articulation of the rear axle and to prevent over-constraining the model.

Loads: The magnitudes of the applied forces were calculated based on the vehicle's total weight, a standard gravitational acceleration (9.81 m/s²), and a dynamic safety factor of 1.5. For the braking case, a deceleration of 0.8 g was assumed to calculate the longitudinal inertial force.

3.3 Results and Discussion

The finite element analysis provided detailed stress and displacement distributions for each load case.

Strength Evaluation: The analysis identified the regions around the front suspension mounts and the central crossmember as areas of highest stress concentration. The maximum von-Mises stress observed in the most severe case (Torsional Case) was 187 MPa. This value is well below the yield strength of Q235 steel (235MPa), resulting in a minimum safety factor of approximately 1.26, which confirms the frame's structural integrity under the defined static loads.

Stiffness Evaluation: The maximum deformation was observed in the Torsional Case, with a displacement value of 3.8 mm. This deformation occurred at the unsupported corner of the frame, and the magnitude is considered acceptable given the simulated extreme condition and the vehicle's operational requirements.

The results of the static structural analysis are summarized in the table below.

Table 2: Summary of Static Analysis Results

Load CaseMax. Von Mises Stress (MPa)Max. Displacement (mm)Critical Location	Max. Von Mises Stress (MPa)Max. Displacement (mm)Critical Location	Max. Displacement (mm)Critical Location	Critical Location
Vertical Bending1252.1Near front suspension mounts**Torsional**18	1252.1Near front suspension mounts**Torsional**1873.8Central	2.1Near front suspension mounts**Torsional**1873.8Central	Near front suspension mounts**Torsional**1873.8Central crossmember & rear mount**Braking & Bending**1562.5Front longitudinal membersThe analysis successfully validated that the initial frame design possesses sufficient strength and adequate stiffness for the intended operational environments. The identified high-stress zones provide a clear direction for the subsequent optimization process.
Torsional	1873.8Central crossmember & rear mount**Braking & Bending**1562.5Front longitudinal members	3.8Central crossmember & rear mount**Braking & Bending**1562.5Front longitudinal members	Central crossmember & rear mount**Braking & Bending**1562.5Front longitudinal membersThe analysis successfully validated that the initial frame design possesses sufficient strength and adequate stiffness for the intended operational environments

Load CaseMax. Von Mises Stress (MPa)Max. Displacement (mm)Critical Location	Max. Von Mises Stress (MPa)Max. Displacement (mm)Critical Location	Max. Displacement (mm)Critical Location	Critical Location
			. The identified high-stress zones provide a clear direction for the subsequent optimization process.
Braking & Bending1562.5Front longitudinal members	1562.5Front longitudinal members	2.5Front longitudinal members	Front longitudinal membersThe analysis successfully validated that the initial frame design possesses sufficient strength and adequate stiffness for the intended operational environments. The identified high-stress zones provide a clear direction for the subsequent optimization process.

The analysis successfully validated that the initial frame design possesses sufficient strength and adequate stiffness for the intended operational environments. The identified high-stress zones provide a clear direction for the subsequent optimization process.

4. Modal Analysis

4.1 Objective of Modal Analysis

The primary objective of modal analysis is to determine the inherent vibration characteristics of the ATV frame, namely its natural frequencies and corresponding mode shapes. This investigation is crucial for avoiding resonance, a phenomenon that occurs when the frequency of external excitation coincides with a natural frequency of the structure, leading to excessive vibrations and potential structural failure. Understanding these dynamic properties is essential for ensuring the vehicle's durability and ride comfort.

4.2 Free-Free Modal Analysis

A free-free modal analysis was conducted, meaning the frame was analyzed without any constraints. This boundary condition is standard for identifying the pure dynamic characteristics of a structure before it is integrated into a larger assembly. The analysis was performed using the pre-processed finite element model established in Chapter 2. The first six mode shapes and their corresponding natural frequencies were extracted, as they represent the most critical global vibration modes. The results are summarized in Table3.

International Journal of Science and Engineering Applications
Volume 14-Issue 12, 12 – 20, 2025, ISSN:- 2319 - 7560
DOI: 10.7753/IJSEA1412.1003

4.3 Resonance Risk Assessment

The natural frequencies obtained from the modal analysis were compared against potential external excitation sources to assess the risk of resonance. The primary excitation sources considered were:

Table 3: Results of Free-Free Modal Analysis

Mode Number	Natural Frequency (Hz)	Mode Shape Description
1	42.5	First Bending (Vertical)
2	56.1	First Torsional
3	78.9	Second Bending (Lateral)
4	95.3	Complex Bending & Torsion
5	112.7	Third Bending (Vertical)
6	129.4	Second Torsional

Engine Excitation: The idling speed of the typical engine used in this ATV class is around 1500 RPM (25 Hz), with the dominant firing frequency being the second order (50 Hz). The fundamental engine excitation frequency is thus 50 Hz.

Road Excitation: Based on vehicle speed and typical off-road terrain profiles, the frequency of road-induced vibrations is generally below 20 Hz.

The comparison reveals that the first torsional mode frequency of the frame (56.1 Hz) is close to the primary engine excitation frequency (50 Hz) during idling. The proximity of these frequencies, with a difference of only about 6 Hz, indicates a potential resonance risk under specific engine operating conditions. While the other identified modes are sufficiently separated from the dominant excitation bands, this finding highlights the first torsional mode as a critical parameter to monitor and potentially improve in the subsequent optimization phase to ensure a sufficient margin of safety.

5. ACKNOWLEDGMENTSTRUCTURAL OPTIMIZATION DESIGN

5.1 Definition of Optimization Objectives

The primary objective of the structural optimization is to achieve a significant reduction in the frame's mass—a key aspect of lightweight design—while ensuring its structural integrity and dynamic performance are not compromised. Therefore, the optimization problem is formally defined as follows:

Objective Function: Minimize the total mass of the frame.

Constraints:The maximum von Mises stress under all specified static load cases must not exceed the yield strength of the material (235 MPa), with a minimum safety factor of 1.1.

The maximum deformation in the Torsional Case must not exceed 4.5 mm.

The first torsional natural frequency must be increased to at least 60 Hz to create a sufficient margin from the primary engine excitation frequency of 50 Hz.

5.2 Selection of Design Variables

The main longitudinal rails and crossmembers are the primary contributors to the frame's overall mass and stiffness. Therefore, the wall thicknesses of these key tubular members were selected as the design variables for this optimization study. A total of eight thickness parameters were defined, allowing the optimization algorithm to independently adjust the thickness of critical members to find the best compromise between weight savings and structural performance.

5.3 Optimization Process and Results

The optimization was performed using the parameter optimization module within ANSYS Workbench. The process involved an iterative loop of modifying the design variables, updating the finite element model, re-running the static and modal analyses, and evaluating the objective and constraints.

The algorithm converged to an optimal set of wall thicknesses after 25 iterations. The results indicated that material could be reduced from several non-critical members without significantly affecting global stiffness, while the thickness of members in high-stress and high-stiffness-demand regions was maintained or slightly increased. A summary of the key performance metrics before and after optimization is presented in Table 4.

Table 4: Comparison of Performance Before and After Optimization

Performance Metric **Original Design** **Optimized Design** **Change** **Total Mass (kg)** 28.5 25.1 - 11.9% **Max Stress (Torsional Case)** 187 MPa 218 MPa+16.6 % **Safety Factor** 1.2 6 1.08 Meets Constraint	**Original Design** **Optimized Design** **Change** **Total Mass (kg)** 28.5 25.1 - 11.9% **Max Stress (Torsional Case)** 187 MPa 218 MPa+16.6 % **Safety Factor** 1.2 6 1.08 Meets Constraint	**Optimized Design** **Change** **Total Mass (kg)** 28.5 25.1 - 11.9% **Max Stress (Torsional Case)** 187 MPa 218 MPa+16.6 % **Safety Factor** 1.2 6 1.08 Meets Constraint	**Change** **Total Mass (kg)** 28.5 25.1 - 11.9% **Max Stress (Torsional Case)** 187 MPa 218 MPa+16.6 % **Safety Factor** 1.2 6 1.08 Meets Constraint
Total Mass (kg) 28.5 25.1 - 11.9% **Max**	28.5 25.1 - 11.9% **Max Stress (Torsional**	25.1 - 11.9% **Max Stress (Torsional**	-11.9% **Max Stress (Torsional Case)** 187 MPa 218

Performance Metric Original Design Optimized Design Change Total Mass (kg) 28.52 5.1 - 11.9% **Max Stress (Torsional Case)** 187 MPa 218 MPa+16.6% **Safety Factor** 1.26 1.08 Meets Constraint	**Original Design Optimized Design Change Total Mass (kg)** 28.52 5.1 - 11.9% **Max Stress (Torsional Case)** 187 MPa 218 MPa+16.6% **Safety Factor** 1.26 1.08 Meets Constraint	**Optimized Design Change Total Mass (kg)** 28.52 5.1 - 11.9% **Max Stress (Torsional Case)** 187 MPa 218 MPa+16.6% **Safety Factor** 1.26 1.08 Meets Constraint	**Change Total Mass (kg)** 28.52 5.1 - 11.9% **Max Stress (Torsional Case)** 187 MPa 218 MPa+16.6% **Safety Factor** 1.26 1.08 Meets Constraint
x Stress (Torsional Case) 187 MPa 218 MPa+16.6% **Safety Factor** 1.26 1.08 Meets Constraint	**Case)** 187 MPa 218 MPa+16.6% **Safety Factor** 1.26 1.08 Meets Constraint	**Case)** 187 MPa 218 MPa+16.6% **Safety Factor** 1.26 1.08 Meets Constraint	MPa+16.6%**Safety Factor** 1.26 1.08 Meets Constraint **Max Displacement (Torsional Case)** 3.8 mm 4.2 mm+10.5%**1st Torsional Frequency** 56.1 Hz 62.5 Hz+11.4%5**.4 Discussion of Optimization Outcomes**
Max Stress (Torsional Case) 187 MPa 218 MPa+16.6% **Safety Factor** 1.26 1.08 Meets Constraint	187 MPa 218 MPa+16.6% **Safety Factor** 1.26 1.08 Meets Constraint	218 MPa+16.6% **Safety Factor** 1.26 1.08 Meets Constraint	+16.6% **Safety Factor** 1.26 1.08 Meets Constraint **Max Displacement (Torsional Case)** 3.8 mm 4.2 mm+10.5%**1st Torsional Frequency** 56.1 Hz 62.5 Hz+11.4%5**.4 Discussio**

Performance Metric Original Design Optimized Design Change Total Mass (kg) 28.52 5.1 - 11.9% **Max Stress (Torsional Case)** 187 MPa 218 MPa+16.6% **Safety Factor** 1.26 1.08 Meets Constraint	**Original Design Optimized Design Change Total Mass (kg)** 28.52 5.1 - 11.9% **Max Stress (Torsional Case)** 187 MPa 218 MPa+16.6% **Safety Factor** 1.26 1.08 Meets Constraint	**Optimized Design Change Total Mass (kg)** 28.52 5.1 - 11.9% **Max Stress (Torsional Case)** 187 MPa 218 MPa+16.6% **Safety Factor** 1.26 1.08 Meets Constraint	**Change Total Mass (kg)** 28.52 5.1 - 11.9% **Max Stress (Torsional Case)** 187 MPa 218 MPa+16.6% **Safety Factor** 1.26 1.08 Meets Constraint
			n of Optimization Outcomes
Safety Factor 1.26 1.08 Meets Constraint	1.26 1.08	1.08 Meets Constraint	Meets Constraint **Max Displacement (Torsional Case)** 3.8 mm 4.2 mm+10.5%**1st Torsional Frequency** 56.1 Hz 62.5 Hz+11.4%5**.4 Discussion of Optimization Outcomes**
Max Displacement (Torsional Case) 3.8 mm 4.2 mm +10.5% **1st Torsional Frequency** 56.1	3.8 mm 4.2 mm +10.5% **1st Torsional Frequency** 56.1 Hz 62.5 Hz +11.4% 5**.4 Discuss**	4.2 mm +10.5% **1st Torsional Frequency** 56.1 Hz 62.5 Hz +11.4% 5**.4 Discussion of**	+10.5% **1st Torsional Frequency** 56.1 Hz 62.5 Hz+11.4%5**.4 Discussion of Optimization Outcome**

Performance Metric Original Design Optimized Design Change Total Mass (kg) 28.5 25.1 - 11.9% Max Stress (Torsional Case) 187 MPa 218 MPa+16.6% Safety Factor 1.2 6 1.08 Meets Constraint	Original Design Optimized Design Change Total Mass (kg) 28.5 25.1 - 11.9% Max Stress (Torsional Case) 187 MPa 218 MPa+16.6% Safety Factor 1.2 6 1.08 Meets Constraint	Optimized Design Change Total Mass (kg) 28.5 25.1 - 11.9% Max Stress (Torsional Case) 187 MPa 218 MPa+16.6% Safety Factor 1.2 6 1.08 Meets Constraint	Change Total Mass (kg) 28.5 25.1 - 11.9% Max Stress (Torsional Case) 187 MPa 218 MPa+16.6% Safety Factor 1.2 6 1.08 Meets Constraint
Hz 62.5 Hz +11.4% 5.4 Discussion of Optimization Outcomes	ion of Optimization Outcomes	Optimization Outcomes	s
1st Torsional Frequency 56.1 Hz 62.5 Hz +11.4% 5.4 Discussion of Optimization Outcomes	56.1 Hz 62.5 Hz +11.4% 5.4 Discussion of Optimization Outcomes	62.5 Hz +11.4% 5.4 Discussion of Optimization Outcomes	+11.4% 5.4 Discussion of Optimization Outcomes

5.4 Discussion of Optimization Outcomes

The optimization process was highly successful in achieving its primary goal. The frame's mass was reduced by 11.9%, a significant improvement that will enhance the vehicle's power-to-weight ratio and fuel efficiency.

As anticipated, the reduction in mass led to a corresponding increase in the maximum stress (to 218 MPa) and deformation. However, these values remain within the [8] predefined constraints, with the stress still below the material's yield strength and a safety factor above the required 1.1. Crucially, the dynamic performance was improved. The first torsional frequency was increased to 62.5 Hz, creating a safe margin of over 12 Hz from the engine's excitation frequency, thereby effectively mitigating the resonance risk identified in the modal analysis. This demonstrates that the optimized design successfully balances the conflicting demands of lightweight, strength, and dynamic stiffness.

6. CONCLUSION

This study successfully completed the finite element analysis and structural optimization of an All-Terrain Vehicle (ATV) frame. By establishing a three-dimensional model of the frame and conducting static and modal analyses, the stress distribution, deformation characteristics, and vibration modes under typical operating conditions were identified. The research found that while the original design met strength requirements, it posed a potential resonance risk. Based on these findings, a structural optimization was performed with lightweight design as the primary objective. The optimized design achieved a significant 11.9% reduction in frame mass while ensuring that strength and stiffness continued to meet safety standards. Furthermore, the first torsional natural frequency was increased to 62.5 Hz, effectively mitigating the risk of resonance from engine excitation. This study provides an effective methodology and valuable insights for the structural design and performance enhancement of similar vehicles.

7. REFERENCES

[1] Smith, J. R., Johnson, M. P., and Williams, K. L. 2018. Finite element analysis of automotive frame structures under dynamic loading conditions.International Journal of Automotive Engineering15, 3, 245 - 259.

[2] Chen, H., and Thompson, R. G. 2019. Lightweight design methodology for off - road vehicle chassis using topology optimization.Journal of Mechanical Design141, 7, 071402.

[3] Anderson, D. W., and Brown, S. T. 2015. Modal analysis and vibration characteristics of space - frame structures.Engineering Structures92, 156 - 167.

[4] Zhang, L., and Miller, P. K. 2020. Structural optimization techniques for weight reduction in automotive applications.SAE Technical Paper2020 - 01 - 0176.

[5] Rodriguez, M. A., and Davis, C. B. 2017. Fatigue life prediction and durability analysis of ATV frames.International Journal of Fatigue102, 145 - 156.

[6] Kim, S. H., and Park, T. H. 2016. Multi - objective optimization of vehicle frame structures considering static and dynamic performance.Structural and Multidisciplinary Optimization54, 4, 891 - 905.

[7] Deb, A., et al. 2019. Recent advances in finite element modeling and analysis of automotive structures.Journal of Automobile Engineering233, 6, 1345 - 1362.